PCCP

Accepted Manuscript

ROYAL SOCIETY OF CHEMISTRY

www.rsc.org/pccp

Physical Chemistry Chemical Physics
CREATED USING THE RSC LaTeX PCCP ARTICLE TEMPLATE – SEE www.rsc.org/electronicfiles FOR DETAILS
ARTICLE TYPE www. rsc.org/xxxxxx | XXXXXXXX

Fundamental frequency from classical molecular dynamics†

Tomonori Yamada[a‡*] **and Misako Aida**[a]

Received Xth XXXXXXXXXX 20XX, Accepted Xth XXXXXXXXX 20XX
First published on the web Xth XXXXXXXXXX 200X
DOI: 10.1039/b000000x

We give a theoretical validation of calculating fundamental frequencies of a molecule from classical molecular dynamics (MD) when its anharmonicity is small enough to be treated by perturbation theory. We specifically give concrete answers to the following questions: (1) What is a proper initial condition of a classical MD to calculate a fundamental frequency? (2) From that condition, how accurately can we extract fundamental frequencies of a molecule? (3) What is the benefit to use ab initio MD for frequency calculations? Our analytical approaches to those questions are classical and quantum normal form theories. As numerical examples we perform two types of MD to calculate fundamental frequencies of H_2O with MP2/aug-cc-pVTZ: one is based on the quartic force field and the other one is direct ab initio MD, where the potential energies and the gradients are calculated on the fly. From those calculations, we show comparisons of the frequencies from MD with the post vibrational self-consistent field calculations, second- and fourth-order perturbation theories, and experiments. We also apply direct ab initio MD to frequency calculations of C–H vibrational modes of tetracene and naphthalene. We conclude that MD can give the same accuracy in fundamental frequency calculation as second-order perturbation theory but the computational cost is lower in large molecules.

1 Introduction

1.1 Computational methodologies for vibrational analysis

Methodologies to treat vibrational states and frequencies beyond the normal mode analysis have been actively investigated for a few decades.[1–14] The vibrational self-consistent field (VSCF) and the advanced methods such as the correlation-corrected VSCF (cc-VSCF), vibrational coupled cluster (VCC) theory and the vibrational (or virtual) configuration interaction (VCI) have been developed[1–8] to obtain the numerical solutions to the time-independent Schrödinger equation with vibrational Hamiltonian. Applicability of VSCF has also been extended to periodic systems taking into account the size consistency of the method by Hirata and co-workers.[11–13] The multiconfiguration time-dependent Hartree method has been developed as a wave-packet-propagation algorithm to solve the time-dependent Schrödinger equation by Meyer and co-workers.[8,14]

Thus, methodology to calculate vibrational eigenstates of molecules or extended systems has been well established, although the computational cost to calculate accurately the full-dimensional potential energy surface (PES) of a middle-sized molecule is enormous. Even though the computational power continues to increase, limitation of system size that can be treated with full-dimensional PES is severe.[8]

An alternative way to approach large systems is to approximate the PES by analytically tractable expression. A typical model PES for anharmonic analysis is the quartic force field (QFF).[1] The analytical expression of QFF is obtained by performing Taylor expansion around the bottom of PES with respect to the normal coordinates and including second-, third-, and fourth-order derivatives of PES. As long as the anharmonicity of the system is small, QFF is accurate for vibrational analysis and useful in terms of computational cost for small or middle sized systems. However, if the system is large, constructing a QFF requires enormous cost since the number of required fourth derivatives of PES increases with the order of n_a^4, where n_a is the number of atoms. It is a severe problem particularly for high level electronic structure calculations such as coupled cluster (CC) where those high order derivatives are expensive to calculate. Therefore, another method to treat vibrational problems is necessary with lower scaling of cost with respect to system size.

Hirata and co-workers developed a quantum Monte Carlo as a new approach to vibrational problems that avoids evaluation of higher-order derivatives of PES.[13]

Another efficient way to predict vibrational spectra we focus attention to is classical molecular dynamics (MD). The main purpose in a series of our works[15,16] is to show the applicability of MD to vibrational problems. The application of

† Electronic Supplementary Information (ESI) available: See DOI: 10.1039/b000000x/

[a] *Center for Quantum Life Sciences and Department of Chemistry, Graduate School of Science, Hiroshima University, Higashi-Hiroshima, 739-8526, Japan.; Tel: +81 82 424 7412; E-mail: tyamada@illinois.edu*
‡ Present address: *Department of Chemistry, University of Illinois at Urbana-Champaign, 600 South Mathews Avenue, Urbana, Illinois 61801, USA.*

MD to vibrational spectroscopy and the problem we aim to solve are addressed bellow.

1.2 Vibrational spectra from MD

MD has widely been used for the treatment of anharmonic vibrational systems.[15–29] Fourier transformation (FT) of trajectories calculated by MD gives vibrational spectra. MD can be used for large systems or even condensed phases. The reason of the low computational cost is that it samples only molecular configurations along the classical trajectory.

There are two important facts to be noted here that allow us to take advantage of MD as a method to calculate vibrational spectra: (1) FT of dipole and polarizability autocorrelation functions correspond to the infrared (IR) and Raman spectra, respectively, the relations of which were shown by Gordon.[30] (2) Another important fact is that, in the case of harmonic oscillators, a quantum correlation function can be accurately calculated from a classical correlation function multiplied by a proper quantum correction, which is so called as detailed balance. Consequently, a classical harmonic frequency is exactly same as the quantum frequency of a harmonic oscillator. Here we define a quantum frequency as the difference of vibrational energies of two eigen states, which corresponds to a peak of an experimental IR or Raman spectrum. A classical frequency is measured as a peak position of a classical vibrational spectrum, i.e. FT of a classical trajectory. We give the detail in next section.

Due to those two facts, MD can be assumed to predict qualitatively comparable IR and Raman spectra with experimentally obtained spectra. Anharmonicity of PES can be treated as a perturbation to a harmonic oscillator if it is small enough. In such a case MD tends to predict qualitatively correct anharmonic frequencies. However, there is no guarantee that a classical anharmonic frequency is quantitatively same as the corresponding quantum frequency in theory without consideration of correspondence between quantum and classical pictures of vibration. Even if a calculated classical frequency agrees well with an experimentally obtained frequency, one cannot deny a possibility that it is just a result of coincidental cancellation of two errors: one is inaccuracy of PES, the other is due to the difference between classical and quantum frequencies.

In recent studies, ab initio MD has been playing an important role for vibrational analysis and has successfully predicted qualitatively experimental spectra.[20–29] However, it is necessary to know how much we can trust such classical frequencies in theory and what is the proper condition of MD to carry out frequency calculations safely.

We pointed out the amount of energy we give in molecules in MD simulation is an important factor to predict correct anharmonic frequencies.[15,16] Helzberg described the relation between a classical frequency and a quantum frequency in his textbook,[31,32] and Marcus and co-workers used the same relation.[33] The relation is that an energy difference between two quantum vibrational states is approximately equal to the classical frequency of the oscillator, whose energy is the average of those two states. We showed how accurately anharmonic frequencies are predicted for di- and tri-atomic molecules with this condition.[15,16] In this article we clarify its theoretically guaranteed accuracy and also show frequency calculations of C–H vibrational modes of naphthalene and tetracene as examples of its application to larger molecules.

1.3 Normal form theory for vibrational problem

In order to combine a classical frequency with a quantum frequency, it is required to express them using the same variables. As far as we know, normal form theory (NFT),[34–45] which has been used in both classical and quantum mechanics, is the most useful method for this purpose and to combine vibrational spectroscopy with MD. In this study we apply NFT as a bridge between those two fields.

A number of works investigating the correspondence between classical and quantum vibrational problems were done based on the EBK quantization[33,46–58] and NFT[34–45] or canonical transformation perturbation theory, since more than 40 years ago. Their focuses were directed toward fundamental dynamical problems, such as high energy states where a primitive technique of NFT or even the theory itself fails.

When we apply NFT to a vibrational problem, a main difficulty we face is the notorious problem of small denominator or the divergence of high order perturbation terms which are generated in the process of performing the techniques of NFT. This is the evidence of the nonintegrability of classical dynamics. Another technical problem of canonical transformation was worked through in order to appropriately scrutinize remnants of invariants buried in a chaotic system.[59,60]

1.4 Classical frequency with a proper condition

In this article, we answer to the following questions: (1) What is a proper initial condition of MD that gives a quantitatively comparable frequency to a quantum frequency? (2) How much accuracy of the frequency can we expect from an MD calculation with that proper initial condition? (3) What is the benefit to use ab initio MD for frequency calculation?

Firstly, in order to answer those three questions, we compare the analytical expressions of classical and quantum frequencies based on NFT. Secondly, we propose a proper initial condition to obtain a frequency, and then compare the classical frequency from that condition with the quantum frequency. As examples of numerical results, we show frequency calculations of water (H_2O), tetracene ($C_{18}H_{12}$), and naphthalene

($C_{10}H_8$) from direct ab initio MD (direct-MD) based on the proper condition. Direct-MD calculates the potential energies and gradients on the fly. We show how much reliable frequencies can be obtained from such calculations.

Note that our approach is completely different from path integral MD or recent semi-classical theory such as SC-IVR method by Wong et. al.,[61] both of which take advantage of a set of classical or semi-classical trajectories to incorporate the delocalized nature of nuclear.

In the following section, we address classical and quantum NFT and frequencies, and show the proper classical condition. In the third section we show how to calculate frequencies from MD. In the fourth section we show the results of frequency calculations of H_2O, $C_{18}H_{12}$, and $C_{10}H_8$. In the last section we summarize our findings.

2 Theory

First, we describe classical and quantum NFT. Even though NFT[34–45] and even the computer programs[56–58] to carry it out have been fully developed by many researchers, it is still necessary to describe it in a specific way that fits our purpose so as to make this article self-explanatory. In the ESI† we also describe briefly the essential parts of classical NFT from the review[37] by Komatsuzaki and Berry, and the quantum NFT from the review[36] by Waalkens and co-workers, with some explanations for our purpose. Secondly, aiming to explicitly express the correspondence between classical and quantum frequencies, we give the analytical forms of frequencies.

2.1 Classical normal form theory

Following the review by Komatsuzaki and Berry,[37] the classical version of NFT or Lie canonical transformation perturbation theory is addressed. Here we apply it to the minimum of PES, while they applied it to the saddle point. We assume that a system possesses the following two characteristics.

First, Hamiltonian is written by a series expansion with respect to a perturbation parameter ε as follows.

$$H = \sum_{i=0}^{\infty} \varepsilon^i H_i \,, \tag{1}$$

where H_0 is the Hamiltonian of a combination of harmonic oscillators given by

$$H_0 = \frac{1}{2}\sum_{i=1}^{N}(p_i^2 + \omega_i^2 q_i^2) \,. \tag{2}$$

Here N is the number of vibrational degrees of freedom, ω_i is the harmonic frequency of mode i, q_i is the mass weighted normal coordinate of mode i, and p_i is the conjugate momentum to q_i. Higher order terms in Eq. (1) are given by

$$H_1 = \frac{1}{6}\sum_{i=1}^{N}\sum_{j=1}^{N}\sum_{k=1}^{N} c_{ijk} q_i q_j q_k \,, \tag{3}$$

$$H_2 = \frac{1}{24}\sum_{i=1}^{N}\sum_{j=1}^{N}\sum_{k=1}^{N}\sum_{l=1}^{N} d_{ijkl} q_i q_j q_k q_l \,, \tag{4}$$

and so on. Here, c_{ijk}, and d_{ijkl} are third and fourth derivatives of PES with respect to normal coordinates. Eq. (1) corresponds to the Taylor expansion of the PES around its minimum. It is also possible to express Hamiltonian using another set of dynamical variables, such as action-angle variables $(J_1,...,J_N,\Theta_1,...,\Theta_N)$, namely,

$$H = \sum_{i=0}^{\infty} \varepsilon^i H_i(J_1,...,J_N,\Theta_1,...,\Theta_N) \,. \tag{5}$$

The ith-action variable is given by

$$J_i = \frac{1}{2\omega_i}(p_i^2 + \omega_i^2 q_i^2) \,. \tag{6}$$

The angle Θ_i is the conjugate variable to J_i, i.e. they satisfy Hamilton's equation of motion. Hereafter a bold variable represents a vector, e.g.

$$\boldsymbol{J} = (J_1,...,J_N) \,. \tag{7}$$

Secondly, the vibrational modes are not in resonance in the system, which ensures that there are N approximately conserved values. Note that we are based on the fact that there are never N strictly conserved values in anharmonic systems because of nonintegrability of multidimensional systems and resonances occur between different vibrational modes after a certain length of time during vibrational motion.[39,49–54] We can assume, however, the existence of N approximately conserved values in a short time, as have been shown before.[49,50] If the energy of a system becomes larger, the number of conserved variables decreases and this approximation becomes more invalid. Since this problem can be an obstacle for its application to large systems, we discuss it in subsections 2.2 and 4.2.

We can transform the original Hamiltonian $H(\boldsymbol{J},\boldsymbol{\Theta})$ into normal form by a canonical transformation. The normal form is defined as follows. When the Hamiltonian is in classical normal form, it is independent from the angle variables $\boldsymbol{\Theta}$.

In accordance with canonical transformation of H, pairs of the dynamical variables, $(\boldsymbol{p},\boldsymbol{q})$ and $(\boldsymbol{J},\boldsymbol{\Theta})$, are also transformed into $(\bar{\boldsymbol{p}},\bar{\boldsymbol{q}})$ and $(\bar{\boldsymbol{J}},\bar{\boldsymbol{\Theta}})$, respectively. The variables with bar are meant to be in classical normal form. When the Hamiltonian is in normal form, the approximately N conserved values are

$$\bar{\boldsymbol{J}} = (\bar{J}_1,...,\bar{J}_N) \,. \tag{8}$$

Although the Hamiltonian of a system given by Eq. (1) is generally not in the normal form, one can obtain the new Hamiltonian $\bar{H}$ in the normal form by means of the canonical transformation at each perturbation order. The transformed new Hamiltonian is expressed as

$$\bar{H}(\bar{\boldsymbol{J}}) = \bar{H}_0(\bar{\boldsymbol{J}}) + \varepsilon^2 \bar{H}_2(\bar{\boldsymbol{J}}) + \varepsilon^4 \bar{H}_4(\bar{\boldsymbol{J}}) + \dots . \tag{9}$$

Here,

$$\bar{H}_0 = \sum_{i=1}^{N} \omega_i \bar{J}_i , \tag{10}$$

$$\bar{H}_2 = \sum_{i=1}^{N}\sum_{j=1}^{N} x_{ij} \bar{J}_i \bar{J}_j , \tag{11}$$

and

$$\bar{H}_4 = \sum_{i=1}^{N}\sum_{j=1}^{N}\sum_{k=1}^{N} y_{ijk} \bar{J}_i \bar{J}_j \bar{J}_k , \tag{12}$$

and so on, where x_{ij} and y_{ijk} are real numbers obtained through the perturbation theory at second- and fourth-order, respectively. The order of $\bar{H}_{2i}$ with respect to $\boldsymbol{J}$ is $i+1$.

According to the canonical perturbation transformation theory, the conserved values $\bar{\boldsymbol{J}}$ are the action variables in normal form given by

$$\bar{J}_i = \frac{1}{2\omega_i}(\bar{p}_i^2 + \omega_i^2 \bar{q}_i^2) , \tag{13}$$

for $i = 1,...,N$ where $\bar{p}_i$ and $\bar{q}_i$ are the new momenta and coordinate of mode i associated with the new Hamiltonian $\bar{H}$. It is easily shown by solving Hamilton's equation of motion that they are given by

$$\bar{p}_i = -\sqrt{2\bar{J}_i \omega_i} \sin\bar{\Theta}_i , \tag{14}$$

and

$$\bar{q}_i = \sqrt{2\bar{J}_i/\omega_i} \cos\bar{\Theta}_i , \tag{15}$$

where $\bar{\Theta}_i$ is given by

$$\bar{\Theta}_i = \bar{\omega}_i t + \beta_i . \tag{16}$$

Here, β_i is initial phase, which is not important in our discussion. Note that $(\bar{J}_i, \bar{\Theta}_i)$ is a pair of conjugate dynamical variables of $\bar{H}$ as well as $(\bar{p}_i, \bar{q}_i)$. Following Hamilton's equation of motion with respect to $\bar{J}_i$ and $\bar{\Theta}_i$, $\bar{\omega}_i$ are also expressed as

$$\dot{\bar{\Theta}}_i = \bar{\omega}_i = \frac{\partial \bar{H}}{\partial \bar{J}_i} . \tag{17}$$

The first equality is from Eq. (16) and the second is from the Hamilton's equation of motion using $\bar{\Theta}_i$ and $\bar{J}_i$. The original Hamiltonian given by Eq. (1) can be transformed by a canonical transformation into the normal form $\bar{H}$ given by Eq. (9). Even though H and $\bar{H}$ represent an anharmonic system, the time dependences of $\bar{p}_i$ and $\bar{q}_i$ that follow $\bar{H}$ are equivalent to those of harmonic oscillators but the frequencies are $\bar{\omega}_i$ not ω_i as seen from Eqs. (14), (15), and (16). $\bar{\omega}_i$ is the anharmonic frequency that are numerically obtained by FT of (q_i, p_i) or $(\bar{q}_i, \bar{q}_i)$ (Eq. (17)) as we describe in the following section.

2.2 Classical frequency

Here, based on classical NFT, we give the definition of classical frequencies $\boldsymbol{\omega}^{\rm cl}$ and the analytical expression. This is the preparation for the later section where we calculate a classical frequency from perturbation theory and from the trajectory which is determined from the peak position of the power spectrum of the momentum.

We can regard $\boldsymbol{p}$ and $\boldsymbol{q}$ as variables obtained by canonical transformation of $\bar{\boldsymbol{p}}$ and $\bar{\boldsymbol{q}}$, respectively. Following the technique described in section I of the ESI† and the review.[37] $\bar{\boldsymbol{p}}$ and $\bar{\boldsymbol{q}}$ are obtained from the canonical transformation, $\hat{T}$, of $\boldsymbol{p}$ and $\boldsymbol{q}$. The reverse transformation, $\hat{T}^{-1}$, of $\bar{\boldsymbol{p}}$ and $\bar{\boldsymbol{q}}$ gives $\boldsymbol{p}$ and $\boldsymbol{q}$.

Performing $\hat{T}^{-1}$ on $\bar{\boldsymbol{p}}$ or $\bar{\boldsymbol{q}}$,

$$p_i = \hat{T}^{-1}\bar{p}_i = \bar{p}_i + \varepsilon(\bar{\boldsymbol{p}}\bar{\boldsymbol{q}})_i^{(2)} + \varepsilon^2(\bar{\boldsymbol{p}}\bar{\boldsymbol{q}})_i^{(3)} + \varepsilon^3(\bar{\boldsymbol{p}}\bar{\boldsymbol{q}})_i^{(4)} + \dots , \tag{18}$$

for $i = 1,...,N$. Here, $(\bar{\boldsymbol{p}}\bar{\boldsymbol{q}})_i^{(l)}$ $(l \geq 2)$ represents a polynomial of $\bar{\boldsymbol{p}}$ and $\bar{\boldsymbol{q}}$, the degree of which is l, e.g., if $l = 2$,

$$(\bar{\boldsymbol{p}}\bar{\boldsymbol{q}})_i^{(2)} = \sum_{j=1}^{N}\sum_{k=1}^{N} (C_i^{(\bar{p}_j\bar{p}_k)} \bar{p}_j\bar{p}_k + C_i^{(\bar{q}_j\bar{p}_k)} \bar{q}_j\bar{p}_k + C_i^{(\bar{q}_j\bar{q}_k)} \bar{q}_j\bar{q}_k) . \tag{19}$$

For q_i, the similar expression to Eq. (18) is obtained:

$$q_i = \bar{q}_i + \varepsilon(\bar{\boldsymbol{p}}\bar{\boldsymbol{q}})_i^{(2)} + \varepsilon^2(\bar{\boldsymbol{p}}\bar{\boldsymbol{q}})_i^{(3)} + \varepsilon^3(\bar{\boldsymbol{p}}\bar{\boldsymbol{q}})_i^{(4)} + \dots , \tag{20}$$

but $(\bar{\boldsymbol{p}}\bar{\boldsymbol{q}})_i^{(j)}$ of Eq. (20) is different from that of Eq. (18). Eqs. (14), (15), (16), and (18) reveal that the power spectrum of p_i yields the peaks at the $\bar{\omega}_i$ and others at the linear combinations of multiple frequencies $n_1\bar{\omega}_1 + \dots + n_N\bar{\omega}_N$, where $(n_1,...,n_N)$ is a set of integers. This is understood as follows. In Eq. (18), time dependencies of $\bar{p}_i$ and $\bar{q}_i$ are given by Eqs. (14)–(16), the frequency of which is $\bar{\omega}_i$, and the term $(\bar{\boldsymbol{p}}\bar{\boldsymbol{q}})^{(l)}$ is a periodic function of $n_1\bar{\omega}_1 + \dots + n_N\bar{\omega}_N$ with

$$\sum_{j=1}^{N} |n_j| = l . \tag{21}$$

For instance, if $l=2$, the first term in Eq. (19) is

$$\begin{aligned} C_2^{(\bar{p}_j\bar{p}_k)}\bar{p}_j\bar{p}_k &= 2C_2^{(\bar{p}_j\bar{p}_k)}\sqrt{J_jJ_k\omega_j\omega_k}\sin\bar{\Theta}_j\sin\bar{\Theta}_k \\ &= -C_2^{(\bar{p}_j\bar{p}_k)}\sqrt{J_jJ_k\omega_j\omega_k} \\ &\quad\times\left(\cos(\bar{\Theta}_j+\bar{\Theta}_k)-\cos(\bar{\Theta}_j-\bar{\Theta}_k)\right) , \end{aligned} \tag{22}$$

and thus the frequencies are $\bar{\omega}_j+\bar{\omega}_k$ and $\bar{\omega}_j-\bar{\omega}_k$.

Among all of peaks in the power spectrum of p_i (or q_i), the intensity of the peak at $\bar{\omega}_i$ must be dominant comparing the combined frequencies, $n_1\bar{\omega}_1+...+n_N\bar{\omega}_N$. It is because $\bar{\omega}_i$ arises from zeroth-order perturbation $\bar{p}_i$ ($\bar{q}_i$) in Eq. (18) (Eq. (20)), whereas their combinations of integral multiples arise from the perturbation terms $\varepsilon^{l-1}(\bar{\boldsymbol{p}}\bar{\boldsymbol{q}})^{(l)}$ ($l\geq 2$). Therefore, we define N principal classical frequencies $(\omega_1^{\rm cl},...,\omega_N^{\rm cl})$ as

$$\omega_i^{\rm cl}=\bar{\omega}_i\ . \tag{23}$$

We do not consider other frequencies $n_1\bar{\omega}_1+...+n_N\bar{\omega}_N$ with small intensity.

Next, we represent $\omega_i^{\rm cl}$ as a function of the action variables in normal form $\bar{J}_i$ for later comparison with a quantum frequency $\omega_i^{\rm qu}$. Using Eqs. (9), (10), (11), (12), (17), and (23), we write the classical frequency of mode i, $\omega_i^{\rm cl}$, as

$$\begin{aligned} \omega_i^{\rm cl} &= \frac{\partial\bar{H}}{\partial\bar{J}_i} \\ &= \omega_i+\varepsilon^2(2x_{ii}\bar{J}_i+2\sum_{j\neq i}^{N}x_{ij}\bar{J}_j) \\ &\quad+\varepsilon^4\left(3y_{iii}\bar{J}_i^2+3\sum_{j\neq i}^{N}(2y_{iij}\bar{J}_i\bar{J}_j+y_{ijj}\bar{J}_j^2)\right. \\ &\quad\left.+3\sum_{j\neq i}^{N}\sum_{k\neq i\cap k\neq j}^{N}y_{ijk}\bar{J}_j\bar{J}_k\right)+... , \end{aligned} \tag{24}$$

where $\sum_{j\neq i}^{N}$ represents summation over j from 1 to N except for the term with $j=i$, and $\sum_{k\neq i\cap k\neq j}^{N}$ is the summation over k but if $k=i$ or $k=j$, the term is not included in the summation. The anharmonic constants x_{ij} and y_{ijk} depend on PES. The anharmonic constants are invariant to swapping the mode indices, i,j,k, etc.

Deriving Eq. (24) is the goal of this subsection. However, before enclosing this subsection, let us address the situation where some of $\bar{\boldsymbol{J}}$ are not constant, i.e. the second assumption we made in the subsection 2.1 breaks down, which is caused by resonances between some of harmonic frequencies:

$$\sum_{i=1}^{N}m_i\omega_i\approx 0\ , \tag{25}$$

where $(m_1,...,m_N)$ are integers. This is more likely to occur particularly in larger systems (i.e. larger N). In such a case, all classical frequencies $\boldsymbol{\omega}^{\rm cl}$ also change in time because they are functions of $\bar{\boldsymbol{J}}$ as seen from Eq. (24). We estimate how significantly this occurs and whether it is meaningful to calculate classical frequencies by monitoring fluctuation of $\boldsymbol{\omega}^{\rm cl}$ along the time evolution in subsection 4.2.

2.3 Quantum normal form theory

Here, we show the analytical expression of the quantum frequency $\omega_i^{\rm qu}$ of an anharmonic oscillator, based on quantum NFT. We then compare it with that of the classical frequency, Eq. (24), given above.

The details of our procedure of the quantum NFT are given in section II of ESI,[†] where we follow the review by Waalkens and co-workers,[36] with some minor modifications so that the obtained result is easily comparable to the classical frequency.

First, let us define the operators of original Hamiltonian $\hat{H}$ and the dynamical variables $\hat{J}_i,\hat{q}_i,\hat{p}_i$ $(i=1,...,N)$:

$$\begin{aligned} \hat{H} &= \frac{1}{2}\sum_{i=1}^{N}(-\hbar^2\frac{\partial^2}{\partial q_i^2}+\omega_i^2q_i^2)+\frac{1}{6}\sum_{i=1}^{N}\sum_{j=1}^{N}\sum_{k=1}^{N}c_{ijk}q_iq_jq_k \\ &\quad+\frac{1}{24}\sum_{i=1}^{N}\sum_{j=1}^{N}\sum_{k=1}^{N}\sum_{l=1}^{N}d_{ijkl}q_iq_jq_kq_l+... , \end{aligned} \tag{26}$$

$$\hat{q}_i=q_i\ , \tag{27}$$

$$\hat{p}_i=-i\hbar\frac{\partial}{\partial q_i}\ , \tag{28}$$

$$\hat{J}_i=\frac{1}{2\omega_i}(-\hbar^2\frac{\partial^2}{\partial q_i^2}+\omega_i^2q_i^2)\ . \tag{29}$$

Note that the PES of $\hat{H}$ is same as the classical system given by Eqs. (2)–(4).

The purpose of the following procedure is to derive the eigen value of vibrational Hamiltonian. In order to do that the original operator of the vibrational Hamiltonian is transformed to the new Hamiltonian operator in quantum normal form.

(Step 1) Transform the operators to the corresponding symbols: $\hat{H}\rightarrow H^{\rm s}$, $\hat{J}_i\rightarrow J_i^{\rm s}$, $\hat{p}_i\rightarrow p_i^{\rm s}$, $\hat{q}_i\rightarrow q_i^{\rm s}$. Symbols represented with the superscript "s" are mathematically more tractable than operators. See subsection 3.1.1 in the review.[36] Like classical variables, the symbols $H^{\rm s}$, $\boldsymbol{J}^{\rm s}$ are the functions of $(\boldsymbol{p}^{\rm s},\boldsymbol{q}^{\rm s})$. In this transformation the resulting functional forms of the symbols $H^{\rm s}(\boldsymbol{p}^{\rm s},\boldsymbol{q}^{\rm s})$, $\boldsymbol{J}^{\rm s}(\boldsymbol{p}^{\rm s},\boldsymbol{q}^{\rm s})$ are same as the classical $H(\boldsymbol{p},\boldsymbol{q})$ and $\boldsymbol{J}(\boldsymbol{p},\boldsymbol{q})$. In addition, since only their functional forms are interested here, there is no need to distinguish $(\boldsymbol{p}^{\rm s},\boldsymbol{q}^{\rm s})$ from $(\boldsymbol{p},\boldsymbol{q})$. Therefore, we represent the symbols in the same way as the classical variables $H(\boldsymbol{p},\boldsymbol{q})$ and $\boldsymbol{J}(\boldsymbol{p},\boldsymbol{q})$.

(Step 2) Transform the symbols $H(\boldsymbol{p},\boldsymbol{q})$ and $\boldsymbol{J}(\boldsymbol{p},\boldsymbol{q})$ into normal form. The direction of transformation is the same as classical normal form: new Hamiltonian in quantum normal form is represented using only $\boldsymbol{J}$. However, the actual mathematical procedure is different from classical case. Because of this, we represent the resulting Hamiltonian in quantum normal form as H' to distinguish it from classical $\bar{H}$. Only its functional form of $H'(\boldsymbol{J})$ is interested here.

$$\begin{aligned} H'(\boldsymbol{J}) &= \sum_{i=1}^{N}\omega_i J_i + \varepsilon^2(\sum_{i=1}^{N}\sum_{j=1}^{N} x_{ij}J_iJ_j + O(\hbar^2)) \\ &\quad +\varepsilon^4\left(\sum_{i=1}^{N}\sum_{j=1}^{N}\sum_{k=1}^{N} y_{ijk}J_iJ_jJ_k \right. \\ &\quad \left. +\frac{\hbar^2}{24}\sum_{i=1}^{N} y_i J_i + O(\hbar^3)\right) + \dots , \end{aligned} \tag{30}$$

where $O(\hbar^2)$ and $O(\hbar^3)$ represent constants of the order of $\hbar^2$ and $\hbar^3$, which cancel in frequency expressions. Note that the coefficients x_{ij} and y_{ijk} are the same as the classical case in Eqs. (11) and (12), but y_i is unique to quantum system. Those unique terms to quantum mechanics arise due to the difference between $\hat{L}_m$ and $\hat{M}_m$ (defined as Eq. (B20) and Eq. (S19) in the ESI†) for the transformations of Hamiltonian.

(Step 3) Transform H' to the corresponding operator: $H' \to \hat{H}'$.

$$\begin{aligned} \hat{H}' &= \sum_{i=1}^{N}\omega_i\hat{J}_i + \varepsilon^2\left(\sum_{i=1}^{N} x_{ii}(\hat{J}_i^2 + \frac{\hbar^2}{4}) \right. \\ &\quad \left. +\sum_{i=1}^{N}\sum_{j\neq i}^{N} x_{ij}\hat{J}_i\hat{J}_j + O(\hbar^2)\right) \\ &\quad +\varepsilon^4\left(\sum_{i=1}^{N} y_{iii}(\hat{J}_i^3 + \frac{5}{4}\hbar^2\hat{J}_i) \right. \\ &\quad +3\sum_{i=1}^{N}\sum_{j\neq i}^{N} y_{iij}(\hat{J}_i^2\hat{J}_j + \frac{1}{4}\hbar^2\hat{J}_j) \\ &\quad +\sum_{i=1}^{N}\sum_{j\neq i}^{N}\sum_{k\neq i\cap k\neq j}^{N} y_{ijk}\hat{J}_i\hat{J}_j\hat{J}_k + \frac{1}{24}\hbar^2\sum_{i=1}^{N} y_i\hat{J}_i \\ &\quad \left. +O(\hbar^3)\right) \\ &\quad +\dots . \end{aligned} \tag{31}$$

Transformation from Eq. (30) to Eq. (31) is performed by using

$$\mathrm{Op}[J_i^{m+1}] = \hat{J}_i\mathrm{Op}[J_i^m] + (\frac{\hbar}{2})^2 m^2 \mathrm{Op}[J_i^{m-1}], \tag{32}$$

$$\mathrm{Op}[J_iJ_j] = \hat{J}_i\hat{J}_j \quad (\text{if } i\neq j), \tag{33}$$

where Op[A] is operator of A (Op[A] $= \hat{A}$). See Eq. (3.98) in literature.[36] Consequently, the Hamiltonian operator in normal form is given by Eq. (31). The terms such as $\hbar^2 x_{ii}/4$ in ε^2 part and $5\hbar^2 y_{iii}\hat{J}_i/4$ in ε^4 part in Eq. (31) do not exist in Eq. (30) or Eq. (9). They are unique to quantum systems.

2.4 Quantum frequency

Since the eigenvalue of $\hat{J}_k$ is $\hbar(v_k+1/2)$, the eigenvalue of $\hat{H}'$ is obtained as follows.

$$\begin{aligned} &E(v_1,\dots,v_N) \\ &= \hbar\sum_{i=1}^{N}\omega_i(v_i+\frac{1}{2}) \\ &+\varepsilon^2\hbar^2\left(\sum_{i=1}^{N} x_{ii}(v_i+\frac{1}{2})^2 + \sum_{i=1}^{N}\sum_{j\neq i}^{N} x_{ij}(v_i+\frac{1}{2})(v_j+\frac{1}{2})\right) \\ &+\varepsilon^4\hbar^3\left(\sum_{i=1}^{N} y_{iii}((v_i+\frac{1}{2})^3 + \frac{5}{4}(v_i+\frac{1}{2})) \right. \\ &+3\sum_{i=1}^{N}\sum_{j\neq i}^{N} y_{iij}((v_i+\frac{1}{2})^2 + \frac{1}{4})(v_j+\frac{1}{2}) \\ &+\sum_{i=1}^{N}\sum_{j\neq i}^{N}\sum_{k\neq i\cap k\neq j}^{N} y_{ijk}(v_i+\frac{1}{2})(v_j+\frac{1}{2})(v_k+\frac{1}{2}) \\ &\left. +\frac{1}{24}\sum_{i=1}^{N} y_i(v_i+\frac{1}{2})\right) + \dots . \end{aligned} \tag{34}$$

Eq. (34) is the well-known formula as the Dunham expansion in the language of vibrational spectroscopy. Consequently, the quantum mechanical frequency or transition energy from $(v_1,\dots,v_i,\dots,v_N)$ to $(v_1,\dots,v_i+1,\dots,v_N)$ is given as follows.

$$\begin{aligned} \omega_i^{\mathrm{qu}} &\equiv \frac{1}{\hbar}\left(E(v_1,\dots,v_i+1,\dots,v_N) - E(v_1,\dots,v_i,\dots,v_N)\right) \\ &= \omega_i + \varepsilon^2\hbar\left(2x_{ii}(v_i+1) + 2\sum_{j\neq i}^{N} x_{ij}(v_j+\frac{1}{2})\right) \\ &\quad +\varepsilon^4\hbar^2\left(y_{iii}(3(v_i+1)^2 + \frac{3}{2}) \right. \\ &\quad +3\sum_{i\neq j}^{N}(2y_{iij}(v_i+1)(v_j+\frac{1}{2}) + y_{jji}(v_j+\frac{1}{2})^2 + \frac{1}{4}y_{jji}) \\ &\quad \left. +3\sum_{j\neq i}^{N}\sum_{k\neq j\cap k\neq i}^{N} y_{ijk}(v_j+\frac{1}{2})(v_k+\frac{1}{2}) + \frac{1}{24}y_i\right) \\ &\quad +\dots . \end{aligned} \tag{35}$$

When ω_i^{qu} is truncated at certain perturbation order $n+1$, we define it as $\omega_i^{\mathrm{qu}(n)}$.

2.5 Condition of classical trajectory for predicting quantum frequency

Since the classical and quantum frequencies are analytically derived, the classical condition can be determined by comparing them with each other. By comparing the second-order terms (ε^2) in Eq. (24) with those in Eq. (35), we can see they are the same with each other if all elements of $\bar{\boldsymbol{J}}$ are set as

$$\bar{J}_i = \hbar(v_i+1)\,, \tag{36}$$

and

$$\bar{J}_j = \hbar(v_j+\frac{1}{2})\,, \tag{37}$$

where i is the particular mode for the energy transition and j represents all of the other modes. Here we define $\omega_i^{\rm cl}[\boldsymbol{v}_i]$ as the ith classical frequency with the condition given by Eqs. (36) and (37). Inserting Eqs. (36) and (37) into Eq. (24),

$$\begin{aligned}\omega_i^{\rm cl}[\boldsymbol{v}_i] \equiv\ & \omega_i+\varepsilon^2\left(2x_{ii}\hbar(v_i+1)+2\sum_{j\neq i}^{N}x_{ij}\hbar(v_j+\frac{1}{2})\right)\\ &+\varepsilon^4\Bigg(3y_{iii}\hbar^2(v_i+1)^2\\ &+3\sum_{j\neq i}^{N}(2y_{iij}\hbar^2(v_i+1)(v_j+\frac{1}{2})+y_{ijj}\hbar^2(v_j+\frac{1}{2})^2)\\ &+3\sum_{j\neq i}^{N}\sum_{k\neq i\cap k\neq i}^{N}y_{ijk}(v_j+\frac{1}{2})(v_k+\frac{1}{2})\Bigg)+\ldots\,.\end{aligned} \tag{38}$$

When $\omega_i^{\rm cl}[\boldsymbol{v}_i]$ is truncated at certain perturbation order $n+1$, we define it as $\omega_i^{{\rm cl}(n)}[\boldsymbol{v}_i]$.

Comparing Eq. (38) with Eq. (35), we see that $\omega_i^{{\rm qu}(2)}$ is equal to $\omega_i^{{\rm cl}(2)}[\boldsymbol{v}_i]$. As non-perturbative approach, numerical comparison is made in the following sections. Such approaches are considered as infinite-order perturbation theory if the methods are accurate. The following conditions are equivalent to Eqs. (36) and (37). (See Eq. (13).)

$$\frac{1}{2}\bar{p}_i(0)^2 = \hbar\omega_i(v_i+1)\,, \tag{39}$$
$$\frac{1}{2}\bar{p}_j(0)^2 = \hbar\omega_j(v_j+\frac{1}{2})\,, \tag{40}$$
$$\frac{1}{2}\bar{q}_i(0)^2 = 0\,, \tag{41}$$
$$\frac{1}{2}\bar{q}_j(0)^2 = 0\,. \tag{42}$$

Here, t in $\bar{\boldsymbol{p}}(t)$ specifies the time t of MD, i.e. $\bar{\boldsymbol{q}}(0)$ and $\bar{\boldsymbol{p}}(0)$ are the initial coordinates and momenta, respectively. $\omega_i^{\rm cl}[\boldsymbol{v}_i]$ is obtained from FT of the trajectory $(\boldsymbol{p},\boldsymbol{q})$ or $(\bar{\boldsymbol{p}},\bar{\boldsymbol{q}})$ with the initial condition expressed by Eqs. (39) – (42).

$\omega_i^{\rm cl}[\boldsymbol{v}_i]$ is guaranteed to have the same accuracy as $\omega_i^{\rm qu}$ in the second-order perturbation theory. In MD calculations, however, the condition (Eqs. (36) and (37) or Eqs. (39) – (42)) cannot be set up strictly, because the canonical transformation $(\bar{\boldsymbol{p}}(0),\bar{\boldsymbol{q}}(0))\leftrightarrow(\boldsymbol{p}(0),\boldsymbol{q}(0))$, which is necessary in actual MD calculations (see next section), are performed perturbatively and the perturbation is needed to be truncated at a certain order. For this reason, we define another classical frequency: $\omega_i^{{\rm cl}(n)[m]}[\boldsymbol{v}_i]$, where the order m specifies the perturbation order for the initial condition to be determined and n is the same as in $\omega_i^{{\rm cl}(n)}[\boldsymbol{v}_i]$. In MD, frequencies are numerically obtained (i.e. $n=\infty$) but the truncation is required in initial condition (i.e. m is finite). $\omega_i^{{\rm cl}(\infty)[m]}[\boldsymbol{v}_i]$ is the one that can be obtained from MD.

The accuracy of $\omega_i^{{\rm cl}(n)[m]}[\boldsymbol{v}_i]$ can be estimated as follows. If the canonical transformation $(\bar{\boldsymbol{p}}(0),\bar{\boldsymbol{q}}(0))\leftrightarrow(\boldsymbol{p}(0),\boldsymbol{q}(0))$ is performed at mth-order, we can only determine the initial condition by

$$\frac{1}{2}\bar{p}_i^{(m)}(0)^2 = \hbar\omega_i(v_i+1)\,, \tag{43}$$
$$\frac{1}{2}\bar{p}_j^{(m)}(0)^2 = \hbar\omega_j(v_j+\frac{1}{2})\,, \tag{44}$$
$$\frac{1}{2}\bar{q}_i^{(m)}(0)^2 = 0\,, \tag{45}$$
$$\frac{1}{2}\bar{q}_j^{(m)}(0)^2 = 0\,, \tag{46}$$

where $\bar{\boldsymbol{p}}^{(m)}(0),\bar{\boldsymbol{q}}^{(m)}(0)$ are in normal forms but within mth-order perturbation theory, i.e.

$$\bar{p}_i^{(m)}(0) = \bar{p}_i(0)+O_{\rm Error}(\varepsilon^{m+1})\,, \tag{47}$$
$$\bar{q}_i^{(m)}(0) = \bar{q}_i(0)+O_{\rm Error}(\varepsilon^{m+1})\,, \tag{48}$$

where $O_{\rm Error}$ indicates the order of error. From Eqs. (13), (47) and (48),

$$\begin{aligned}\bar{J}_i^{(m)} &\equiv \frac{1}{2\omega_i}\left(\bar{p}_i{}^{(m)2}+\omega_i^2\bar{q}_i^{(m)2}\right) &(49)\\ &= \bar{J}_i+O_{\rm Error}(\varepsilon^{m+1})\,, &(50)\end{aligned}$$

for $i=1,\ldots,N$. Accordingly, the accuracy of the frequency from such an approximated condition can be estimated as

$$\omega_i^{{\rm cl}(n)[m]}[\boldsymbol{v}_i]=\omega_i^{{\rm cl}(n)}[\boldsymbol{v}_i]+O_{\rm Error}(\varepsilon^{m+3})\,, \tag{51}$$

as can be seen by inserting Eq. (50) into Eq. (24). Note that in MD the frequency is not truncated, which means we can assume it as the case of $n=\infty$.

3 Calculations

We show frequency calculations of H_2O, $C_{18}H_{12}$, and $C_{10}H_8$. The main purpose of H_2O calculation is to show accuracy of

$\omega_i^{\mathrm{cl}(n)}[\boldsymbol{\nu}_i]$ comparing with ω_i^{qu} precisely at several perturbation orders n: zeroth-, second-, and fourth-orders. Zeroth-order frequency is the harmonic frequency. Second- and fourth-order frequencies can be calculated following Eq. (35) and Eq. (38), once the anharmonic coefficients x and y are calculated by a canonical transformation. While analytical expressions are available for them, the infinite order frequencies may be obtained by non-perturbative method. We assume that the quantum frequencies that are numerically obtained by cc-VSCF and VCI have the accuracy of infinite order perturbation theory. We also perform MD calculations and see the accuracy of $\omega_i^{\mathrm{cl}(\infty)[m]}[\boldsymbol{\nu}_i]$ with $m = 0, 4$. In addition, we check the effect of difference between QFF and direct PES on frequency by using those two types of PES in MD, cc-VSCF and VCI. For PES, MP2/aug-cc-pVTZ level of theory is used for electronic structure calculations. We show the overview of the whole procedure in Fig. 1.

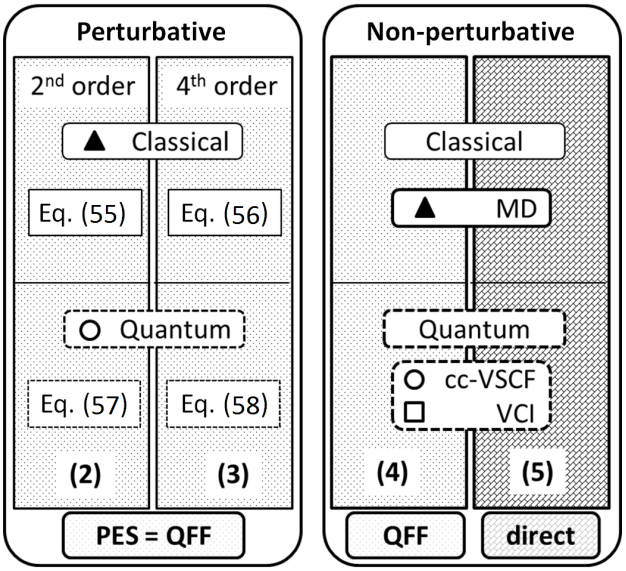

Fig. 1 Overview of the whole frequency calculations of H_2O. We calculate vibrational frequencies based on second-order and fourth-order perturbation theories (left) using QFF, and non-perturbative approaches (right) with MD and post-VSCF using QFF or direct PES (darker-shaded area), and also classically and quantum mechanically. See text for details. The symbols (open square, open circle and filled triangle) designated to methods are the same as in Fig. A in the ESI,† and the numbers in parentheses are also used in the same way as those used in Fig. A and Table 1.

Calculations of $C_{18}H_{12}$ and $C_{10}H_8$ are meant to be tests of MD as a practical vibrational analysis for larger systems. It is expected in general that an accurate calculation of a classical frequency with the proposed condition (Eqs. (39)–(42) or Eqs. (43)–(46)) is difficult because of the following reason. The number of resonances between modes increases with the system size. The more significantly resonances occur, the assumption that approximately N conserved values exist becomes more invalid. If the resonance occurs, the spectrum becomes blur and the peaks shift along time evolution gradually. In such a case it is difficult to assign a frequency in the spectrum, and the classical condition we set up breaks down. We can know how significantly such resonances occur by checking time evolution of power spectra.

We calculate direct PES with HF/STO-3G, the accuracy of which is far from required accuracy to be compared with experimental values. However, comparison with the quantum frequency with the same electronic structure calculation is meaningful. The reason for choosing HF/STO-3G as electronic structure calculation is limitation of the computational cost.

3.1 Frequencies of H_2O from perturbation theory

For the second- and fourth-order perturbation theories, we use QFF PES given by

$$V(q_1,q_2,q_3) = \frac{1}{2}\sum_{i=1}^{3}\omega_i^2 q_i^2 + \frac{1}{6}\sum_{i=1}^{3}\sum_{j=1}^{3}\sum_{k=1}^{3} c_{ijk}q_iq_jq_k + \frac{1}{24}\sum_{i=1}^{3}\sum_{j=1}^{3}\sum_{k=1}^{3}\sum_{l=1}^{3} d_{ijkl}q_iq_jq_kq_l \,. \quad (52)$$

Therefore, the first and second-order perturbation terms of Hamiltonian are given by

$$H_1 = \frac{1}{6}\sum_{i=1}^{3}\sum_{j=1}^{3}\sum_{k=1}^{3} c_{ijk}q_iq_jq_k \,, \quad (53)$$

and

$$H_2 = \frac{1}{24}\sum_{i=1}^{3}\sum_{j=1}^{3}\sum_{k=1}^{3}\sum_{l=1}^{3} d_{ijkl}q_iq_jq_kq_l \,. \quad (54)$$

For classical frequencies, from Eq. (38) with $\boldsymbol{\nu}_i = \mathbf{0}_i$ (all of $(\nu_1,\ldots,\nu_N)$ are zero in Eqs. (36) and (37)), we obtain the second- and fourth-order frequencies:

$$\omega_i^{\mathrm{cl}(2)}[\mathbf{0}_i] = \omega_i + \varepsilon^2\hbar\left(2x_{ii} + \sum_{j\neq i}^{3} x_{ij}\right) \,, \quad (55)$$

and

$$\omega_i^{\mathrm{cl}(4)}[\mathbf{0}_i] = \omega_i^{\mathrm{cl}(2)}[\mathbf{0}_i] + \varepsilon^4\hbar^2\left(3y_{iii} + 3\sum_{j\neq i}^{3}(y_{iij} + \frac{1}{4}y_{ijj}) + \frac{3}{4}\sum_{j\neq i}^{3}\sum_{k\neq i\cap k\neq i}^{3} y_{ijk}\right) \,. \quad (56)$$

Quantum frequencies are written in the same way. If $\boldsymbol{v} = \boldsymbol{0}$ in Eq. (35), the second- and fourth-order fundamental quantum frequencies for the transition $(0,...,0,...,0) \rightarrow (0,...,1,...,0)$, where the transition occurs in mode i, are obtained as follows:

$$\omega_i^{\mathrm{qu}(2)} = \omega_i + \varepsilon^2\hbar\left(2x_{ii} + \sum_{j\neq i}^{3} x_{ij}\right) , \quad (57)$$

and

$$\omega_i^{\mathrm{qu}(4)} = \omega_i^{\mathrm{qu}(2)} + \varepsilon^4\hbar^2\left(\frac{9}{2}y_{iii} + 3\sum_{j\neq i}^{3}(y_{iij} + \frac{1}{2}y_{ijj}) + \frac{3}{4}\sum_{j\neq i}^{3}\sum_{k\neq i\cap k\neq i}^{3} y_{ijk} + \frac{1}{24}y_i\right) . \quad (58)$$

We calculate the coefficients x_{ij}, y_{ijk}, and y_i following the procedures written in subsection I-2 and section II in the ESI†. See also literatures[36,37] concerning the details. x_{ij}, y_{ijk}, and y_i depend on the harmonic frequencies, ω_i, and the force constants, c_{ijk}, and d_{ijkl}. The force constants are obtained at the MP2/aug-cc-pVTZ level of theory using the GAMESS package.[62,63]

3.2 Frequencies of H_2O from non-perturbative approach

Here, we show how to calculate $\omega_i^{\mathrm{cl}(\infty)[m]}[\boldsymbol{0}_i]$ with $m = 0, 4$ from FT of $p_i(t)$ from the MD trajectory. We use two types of PES to generate dynamics. The first one is QFF PES given by Eq. (52), and the second one is direct PES.

To set up the conditions given by Eqs. (43)–(46), we perform the following procedure.

Step 1: The molecular structure is optimized by means of ab initio MO with the theoretical level of MP2/aug-cc-pVTZ.

Step 2: Normal mode analysis of the optimized geometry is performed, and the harmonic frequencies $\boldsymbol{\omega}$ are obtained. The normal coordinates and conjugate momenta are expressed in terms of the Cartesian coordinates $\boldsymbol{r}$, namely,

$$\boldsymbol{r} = \boldsymbol{L}\boldsymbol{q} , \quad (59)$$

and

$$\dot{\boldsymbol{r}} = \boldsymbol{L}\boldsymbol{p} , \quad (60)$$

where $\boldsymbol{L}$ is a matrix obtained from normal mode analysis, and $\boldsymbol{r}$ and $\dot{\boldsymbol{r}}$ represent the position and velocity, respectively, in Cartesian coordinates. In addition, the cubic and quartic potential energy coefficients c_{ijk} and d_{ijkl} are obtained at the optimized geometry.

Step 3: The initial values of $\bar{\boldsymbol{p}}^{(m)}$ and $\bar{\boldsymbol{q}}^{(m)}$ are determined from Eqs. (43)–(46) using the harmonic frequencies $\boldsymbol{\omega}$ calculated in *Step* 1.

Step 4: By means of the canonical transformation, the original dynamical variables are expressed in terms of the transformed variables, namely,

$$\boldsymbol{p} = \boldsymbol{p}(\bar{\boldsymbol{p}}^{(m)}, \bar{\boldsymbol{q}}^{(m)}) , \quad (61)$$

$$\boldsymbol{q} = \boldsymbol{q}(\bar{\boldsymbol{p}}^{(m)}, \bar{\boldsymbol{q}}^{(m)}) . \quad (62)$$

The initial conditions determined for $\bar{\boldsymbol{p}}^{(m)}$ and $\bar{\boldsymbol{q}}^{(m)}$ by Eqs. (43)–(46) are expressed with respect to $(\boldsymbol{r}, \dot{\boldsymbol{r}})$ using Eqs. (59)–(62) for MD calculations. The *Step* 4 is not necessary when $m = 0$, since

$$\boldsymbol{p} = \bar{\boldsymbol{p}}^{(0)} , \quad (63)$$

$$\boldsymbol{q} = \bar{\boldsymbol{q}}^{(0)} . \quad (64)$$

Trajectories are calculated by integrating Newton's equation of motion with energies and forces obtained from QFF (QFF-MD) or directly from ab initio molecular orbital theory at each time step (direct-MD) with the theory of MP2/aug-cc-pVTZ. We need to point out that in direct-MD the dynamics is generated directly, but the canonical transformation to define the initial conditions in *Step* 4 is performed with QFF if $m > 0$. The effect of using QFF PES for canonical transformation but generating dynamics direct PES is discussed in the result section. The classical nuclear trajectories are integrated with a constant total energy using a fourth-order Gear predictor–corrector algorithm;[64] a time step of 0.1 fs is used to ensure the numerical accuracy. The total number of steps is 5000 for each trajectory calculation. We used the HONDO2004 program.[65]

Three trajectories are run in order to obtain three frequencies of different modes of H_2O with the different initial conditions.

As non-perturbative approach to obtain $\omega^{\mathrm{qu}(\infty)}$, cc-VSCF calculations are performed using GAMESS program package.[62,63] The PES used for cc-VSCF calculations and the level of electronic structure calculation are the same as those used in the MD calculations.

3.3 Frequencies of $C_{18}H_{12}$ and $C_{10}H_8$

For $C_{18}H_{12}$ and $C_{10}H_8$, we calculate $\omega_i^{\mathrm{cl}(\infty)[0]}[\boldsymbol{0}_i]$ and compare it with $\omega_i^{\mathrm{qu}(2)}$. Direct-MD is performed for generating dynamics. The electronic structure calculations are done with HF/STO-3G. The force constants and the second-order perturbation theory for quantum frequencies are carried out using Gaussian09 program package.[66]

In order to obtain N frequencies of different modes, N trajectories are run with different initial conditions.

4 Results and discussion

4.1 H_2O

The obtained classical and quantum frequencies are shown in Table 1 and also plotted in Fig. A in the ESI†. (Hereafter $[\mathbf{0}_i]$ and i in $\omega_i^{\mathrm{cl}(n)}[\mathbf{0}_i]$ and ω_i^{qu} are abbreviated.) One of the trajectories is shown in Fig. B in the ESI† as example.

Classical and quantum frequencies agree within second-order perturbation theory as addressed in subsection 3.5 with the classical condition therein. They are compared with each other in fourth- and infinite-orders to see the deviations.

In Table 1 the zeroth-order frequencies (1) are the harmonic frequencies, and analytical expressions of second-order frequencies (2) $\omega^{\mathrm{qu}(2)}$ and $\omega^{\mathrm{cl}(2)}$ are given by Eqs. (57) and (55), and fourth-order frequencies (3) $\omega^{\mathrm{qu}(4)}$, $\omega^{\mathrm{cl}(4)}$ are given by Eqs. (58) and (56), respectively. In non-perturbative approaches (5), cc-VSCF is used in this work for $\omega^{\mathrm{qu}(\infty)}$ and MD is used for $\omega^{\mathrm{cl}(\infty)[4]}$. $\omega^{\mathrm{cl}(\infty)[0]}$ is also shown taken from our previous calculations.[16] Experimental values[67] (6) are also shown.

First, let us discuss perturbative calculations (1)–(3). The $\omega^{\mathrm{qu}(2)}$ and $\omega^{\mathrm{cl}(2)}$ are the same in the condition of Eqs. (36) and (37). The fourth-order frequencies $\omega^{\mathrm{qu}(4)}$ and $\omega^{\mathrm{cl}(4)}$ are no longer the same. Nonetheless, the differences between them are very small: $\omega^{\mathrm{qu}(4)} - \omega^{\mathrm{cl}(4)}$ = 20 cm^{-1}, -2 cm^{-1}, and -7 cm^{-1} for the symmetric stretching, bending, and antisymmetric stretching vibrational modes, respectively.

Next, we discuss non-perturbative approaches (4,5). In MD, there are two complications as to the level of accuracy: first, even though MD is a non-perturbative approach, the initial condition is determined based on the perturbative canonical transformation. Second, in direct-MD (5), the qualities of PES are different between initial condition (QFF) and dynamics (direct). The clue to estimate the accuracy is Eqs. (47)–(51): the error comes from truncation of canonical transformation (ε^{m+1}) for initial condition gives a smaller error (ε^{m+3}) in the frequency. Therefore we can say that $\omega^{\mathrm{cl}(\infty)[4]}$ from QFF MD (4) are as accurate as $\omega^{\mathrm{cl}(6)}$. In the same sense, using QFF PES for canonical transformation in the initial condition determining process gives a smaller error in frequency than using it for dynamics.

Similar to the fourth-order perturbation theory, the differences between $\omega^{\mathrm{qu}(\infty)}$ from cc-VSCF and $\omega^{\mathrm{cl}(\infty)[4]}$ with QFF PES are $\omega^{\mathrm{qu}(\infty)} - \omega^{\mathrm{cl}(\infty)[4]} = 11\ \mathrm{cm}^{-1}, -1\ \mathrm{cm}^{-1}$, and $-1\ \mathrm{cm}^{-1}$, and with direct PES: $\omega^{\mathrm{qu}(\infty)} - \omega^{\mathrm{cl}(\infty)[4]}$ = 3 cm^{-1}, -30 cm^{-1}, and -33 cm^{-1}, for the symmetric stretching, bending, and antisymmetric stretching modes, respectively. Those differences are possibly due to inaccuracy of cc-VSCF not MD because if the more reliable direct-VCI is used as $\omega^{\mathrm{qu}(\infty)}$, the differences are smaller. From literature,[2] $\omega^{\mathrm{qu}(\infty)}$ values are 3647 cm^{-1}, 1576 cm^{-1}, and 3760 cm^{-1}, and $\omega^{\mathrm{qu}(\infty)} - \omega^{\mathrm{cl}(\infty)[4]}$ = 4 cm^{-1}, -1 cm^{-1}, and -17 cm^{-1}, for the symmetric stretching, bending, and antisymmetric stretching modes, respectively.

Table 1 Fundamental frequencies ($\omega^{\mathrm{qu}(n)}$, $\omega^{\mathrm{cl}(n)}$, $\omega^{\mathrm{cl}(n)[m]}$) of H_2O in cm^{-1}. Non-perturbative approaches are used for $n = \infty$. The level of electronic structure calculations is MP2/aug-cc-pVTZ.

Symmetric stretching				
PES[a]	Quantum		Classical	
(1) –	$\omega^{\mathrm{qu}(0)}$	3800	$\omega^{\mathrm{cl}(0)}$	3800
(2) QFF	$\omega^{\mathrm{qu}(2)}$	3643	$\omega^{\mathrm{cl}(2)}$	3643
(3) QFF	$\omega^{\mathrm{qu}(4)}$	3685	$\omega^{\mathrm{cl}(4)}$	3665
(4) QFF	$\omega^{\mathrm{qu}(\infty)}$	3687[b]	$\omega^{\mathrm{cl}(\infty)[4]}$	3676
(5) Direct	$\omega^{\mathrm{qu}(\infty)}$	3646[b]	$\omega^{\mathrm{cl}(\infty)[0]}$	3640[d]
(5) Direct	$\omega^{\mathrm{qu}(\infty)}$	3647[c]	$\omega^{\mathrm{cl}(\infty)[4]}$	3643
(6) Experimental		3657[e]		
Bending				
PES[a]	Quantum		Classical	
(1) –	$\omega^{\mathrm{qu}(0)}$	1626	$\omega^{\mathrm{cl}(0)}$	1626
(2) QFF	$\omega^{\mathrm{qu}(2)}$	1565	$\omega^{\mathrm{cl}(2)}$	1565
(3) QFF	$\omega^{\mathrm{qu}(4)}$	1556	$\omega^{\mathrm{cl}(4)}$	1558
(4) QFF	$\omega^{\mathrm{qu}(\infty)}$	1556[b]	$\omega^{\mathrm{cl}(\infty)[4]}$	1557
(5) Direct	$\omega^{\mathrm{qu}(\infty)}$	1547[b]	$\omega^{\mathrm{cl}(\infty)[0]}$	1578[d]
(5) Direct	$\omega^{\mathrm{qu}(\infty)}$	1576[c]	$\omega^{\mathrm{cl}(\infty)[4]}$	1577
(6) Experimental		1595[e]		
Antisymmetric stretching				
PES[a]	Quantum		Classical	
(1) –	$\omega^{\mathrm{qu}(0)}$	3923	$\omega^{\mathrm{cl}(0)}$	3923
(2) QFF	$\omega^{\mathrm{qu}(2)}$	3743	$\omega^{\mathrm{cl}(2)}$	3743
(3) QFF	$\omega^{\mathrm{qu}(4)}$	3787	$\omega^{\mathrm{cl}(4)}$	3794
(4) QFF	$\omega^{\mathrm{qu}(\infty)}$	3787[b]	$\omega^{\mathrm{cl}(\infty)[4]}$	3788
(5) Direct	$\omega^{\mathrm{qu}(\infty)}$	3744[b]	$\omega^{\mathrm{cl}(\infty)[0]}$	3751[d]
(5) Direct	$\omega^{\mathrm{qu}(\infty)}$	3760[c]	$\omega^{\mathrm{cl}(\infty)[4]}$	3777
(6) Experimental		3756[e]		

[a] The numbering of methods (1)–(6) is consistent with Fig. 1 and Fig. A in the ESI†. [b] From cc-VSCF. [c] From VCI.[1] [d] From previous work.[16] [e] The experimental values.[67]

From Fig. A in the ESI,† we can say that quantum and classical frequencies converge as increasing order of perturbation theory (1)–(4), but slightly changes if PES is changed to direct (5). Results from direct-MD and direct-VCI are more close to the experimental values (5) than from QFF-MD and cc-VSCF with QFF PES, respectively.

In practical point of view, however, $\omega^{\mathrm{cl}(\infty)[0]}$ is much easier to calculate than $\omega^{\mathrm{cl}(\infty)[4]}$ from MD, because $\omega^{\mathrm{cl}(\infty)[0]}$ requires only normal mode analysis to determine the initial condition whereas $\omega^{\mathrm{cl}(\infty)[4]}$ requires higher order force constants and performing the canonical transformation. $\omega^{\mathrm{cl}(\infty)[0]}$ from direct-MD also well agrees with $\omega^{\mathrm{qu}(\infty)}$ from direct-VCI: $\omega^{\mathrm{qu}(\infty)} - \omega^{\mathrm{cl}(\infty)[0]} = 7\ \mathrm{cm}^{-1}, -2\ \mathrm{cm}^{-1}$, and $9\ \mathrm{cm}^{-1}$. The differences of $\omega^{\mathrm{cl}(\infty)[0]}$ from experimental values are also small: 17 cm^{-1}, 17

cm^{-1}, and 5 cm^{-1}.

Summarizing the results of H_2O, quantum and classical frequencies are close to each other by applying the proper condition given by Eqs. (36)–(37). Even in higher orders of perturbation, the agreement is reasonable.

4.2 $C_{18}H_{12}$ and $C_{10}H_8$

Direct-MD calculations of $C_{18}H_{12}$ and $C_{10}H_8$ are carried out based on the condition Eqs. (39)–(42) with $m = 0$:

$$\frac{1}{2}\bar{p}_i^{(0)}(0)^2 = \hbar\omega_i(v_i+1)\,, \quad (65)$$

$$\frac{1}{2}\bar{p}_j^{(0)}(0)^2 = \hbar\omega_j(v_j+\frac{1}{2})\,, \quad (66)$$

$$\frac{1}{2}\bar{q}_i^{(0)}(0)^2 = 0\,, \quad (67)$$

$$\frac{1}{2}\bar{p}_j^{(0)}(0)^2 = 0\,. \quad (68)$$

In order to calculate N frequencies of different modes, N trajectories are run with different initial conditions, i.e. different i in Eqs. (65)–(68). From each trajectory, $\omega^{\mathrm{cl}(\infty)[0]}$ is calculated, and it is compared with $\omega^{\mathrm{qu}(2)}$ calculated by second-order perturbation theory (2PT). Note that direct PES is used for $\omega^{\mathrm{cl}(\infty)[0]}$ but QFF is used for $\omega^{\mathrm{qu}(2)}$. The level of electronic structure calculation is HF/STO-3G.

We calculate 4 C–H stretching modes of $C_{18}H_{12}$ and 8 C–H stretching modes of $C_{10}H_8$ as shown in Figs. 2 and 3, respectively. In each MD calculation, since energies are given to all vibrational modes in each trajectory, there are several peaks in each spectrum. In order to extract the peak corresponding to ith mode, the trajectory needs to be projected to the ith normal mode. We project the MD trajectories to the quasi-normal coordinates as defined bellow, instead of rigorous projection to normal coordinates, which is cumbersome in such large molecules. The time derivative of quasi-normal coordinate Q_i is defined as:

$$\frac{dQ_i}{dt} = \sum_{j=1}^{N_{\mathrm{C-H}}} s_{ij}\frac{dr_j}{dt}\,, \quad (69)$$

where r_j is jth C–H bond length, $N_{\mathrm{C-H}}$ is the number of C–H bonds, s_{ij} is either $+1$ or -1 depending on the direction of ith C–H bond vibration contributing to the quasi-normal mode Q_i. See Figs. 2 and 3.

Power spectra are obtained from FT of $\dot{Q}_i$. The power spectra of $C_{18}H_{12}$ are shown in Figs. 4–7 from the MD calculations with initial conditions for 1–4 mode frequencies, respectively. The power spectra of $C_{10}H_8$ are shown in the ESI.† The spectra in each figure were obtained from three time-windows of the same trajectory: 0.0 – 0.5 ps, 0.1 – 0.6 ps, and 0.2 – 0.7 ps. Each time-window has 0.5 ps length of time,

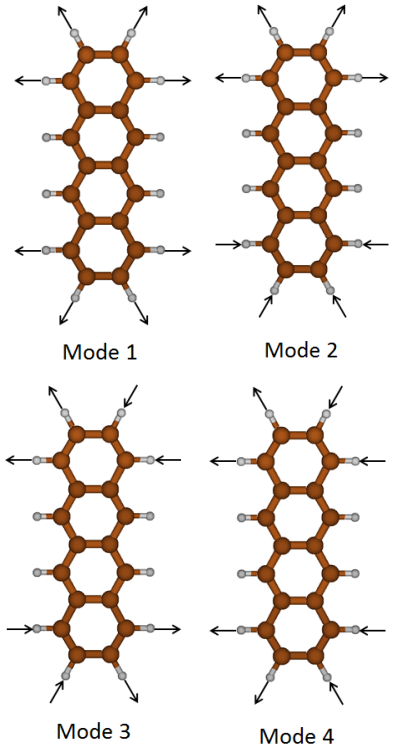

Fig. 2 C–H vibrational modes 1 to 4 of $C_{18}H_{12}$, which are calculated by MD. The labels of modes are numbered from the highest harmonic frequencies.

FT of which gives 67 cm^{-1} intervals between the neighboring discrete values in frequency domain. In order to make the intervals smaller, we put zero as fictitious data outside of the 0.5 ps time-windows and make the time length 13 ps which gives 1.3 cm^{-1} of intervals. This procedure does not affect the positions of the major peaks, but gives small artificial oscillations on the feet of peaks due to the discontinuous change in time domain at the edge of the time-window.

We consider the top of the main peaks in spectra from time windows of 0.0 – 0.5 ps as the classical frequencies calculated with the condition given by Eqs. (65)–(68) as indicated by black arrows in Figs 4–7. After a certain time of dynamics, classical frequencies generally shift to lower or higher frequency region because of the resonance between modes. If the peak is widely shifted, the corresponding frequency is no longer equivalent to the one calculated from Eqs. (65)–(68) and the calculated frequency may not be comparable to quantum frequency. We estimate the magnitude of a peak shift during dynamics by calculating

$$\Delta\omega \equiv \left[\frac{1}{2}\left((\omega_{0.0-0.5}-\omega_{0.1-0.6})^2 + (\omega_{0.0-0.5}-\omega_{0.2-0.7})^2\right)\right]^{\frac{1}{2}}, \quad (70)$$

where $\omega_{t_1-t_2}$ is the peak position of spectrum in the time-window (t_1 ps – t_2 ps). For instance, $\omega_{0.0-0.5}$ is indicated by the black arrow in each power spectrum.

From Fig. 5 and Fig. 7, we can see that the classical condition to calculate the corresponding frequencies (mode 2 and 4, respectively) are well conserved, because the shapes of spectra are similar in the three time-windows. Validity of mode 3 calculation in Fig. 6 is questionable even at 0.0 – 0.5 ps, because the spectrum of initial time window is already split in multiple peaks. The split is likely due to resonances between vibrational modes. It also occurs in mode 1 calculation in Fig. 4 after 0.5 ps.

We show the frequencies of those peaks with $\Delta\omega$ in Table 2 (also shown by arrows in Figs. 4–7). The differences between $\omega_i^{\mathrm{qu}(2)}$ and $\omega_i^{\mathrm{cl}(\infty)[0]}$ are small (-7, -14, -2 cm^{-1}) in modes 1, 2, and 4. That the difference in mode 3 is large is accounted for by the fact that $\Delta\omega$ is large and $\omega_3^{\mathrm{cl}(\infty)[0]}$ is not reliable.

Table 2 Frequencies of $C_{18}H_{12}$ in cm^{-1}. The level of electronic structure calculations is HF/STO-3G.

Mode	Harmonic	$\omega^{\mathrm{qu}(2)}$	$\omega^{\mathrm{cl}(\infty)[0]}(\pm\Delta\omega)$	$\omega^{\mathrm{qu}(2)}-\omega^{\mathrm{cl}(\infty)[0]}$
1	3742	3640	3647($\pm$52)	-7
2	3742	3663	3677($\pm$3)	-14
3	3735	3641	3599($\pm$113)	42
4	3735	3654	3656($\pm$10)	-2

In the same way, the classical frequencies are obtained for $C_{10}H_8$. The obtained spectra are shown section V in the ESI and the frequencies are given in Table 3. Even though $\Delta\omega$ are small in modes 1–3, the difference between $\omega^{\mathrm{qu}(2)}$ and $\omega^{\mathrm{cl}(\infty)[0]}$ is relatively larger in $C_{10}H_8$ comparing $C_{18}H_{12}$ and H_2O. Possible factors of these disagreements are the inherent error $O(\varepsilon^3)$ in MD calculation (Eq. (51)) and the difference of QFF in 2PT and direct PES in MD. Because of those factors, we cannot conclude which is more reliable. As long as $\Delta\omega$ is small, $\omega^{\mathrm{cl}(\infty)[0]}$ is considered to be comparable to $\omega^{\mathrm{qu}(2)}$.

Table 3 Frequencies of $C_{10}H_8$ in cm^{-1}. The level of electronic structure calculation is HF/STO-3G.

Mode	Harmonic	$\omega^{\mathrm{qu}(2)}$	$\omega^{\mathrm{cl}(\infty)[0]}(\pm\Delta\omega)$	$\omega^{\mathrm{qu}(2)}-\omega^{\mathrm{cl}(\infty)[0]}$
1	3744	3649	3705($\pm$4)	-56
2	3743	3663	3684($\pm$10)	-21
3	3735	3652	3680($\pm$7)	-28
4	3735	3656	3702($\pm$18)	-46
5	3721	3620	3615($\pm$98)	5
6	3720	3639	3686($\pm$29)	-47
7	3712	3612	3666($\pm$29)	-54
8	3707	3599	3490($\pm$119)	-109

Second-order perturbation theory or post-VSCF methods are efficient by taking advantage of QFF PES. However constructing QFF requires enormous costs for large systems, and direct-MD is more efficient in such cases. The total number of fourth-order force constant (d_{ijkl}) is ${}_{3n_a-6}C_4$ (if indices (i,j,k,l) are different). For $C_{18}H_{12}$ this number is 1929501 ($n_a = 30$). Direct-MD requires $(3n_a-6)N_{\mathrm{step}}$ energy and gradient calculations (420000 for $C_{18}H_{12}$), if all modes' frequencies are calculated, where N_{step} is the number of time step and is 5000 in our analysis. Thus, for such a large system as $C_{18}H_{12}$ direct-MD has advantage in computational cost over 2PT using QFF.

5 Conclusion

We determined the proper initial condition Eqs. (39) – (42) for MD to calculate fundamental frequency, based on classical and quantum normal form theories. Because of the similarity between the classical Hamiltonian and the quantum Hamiltonian operator in normal form, the classical frequency in that condition is equivalent to the quantum frequency (fundamental frequency) within the second-order perturbation theory.

In the case of H_2O calculations, we found that (1) the agreement between classical and quantum frequencies are good in fourth-order perturbation theory and non-perturbative approaches using MD and post-VSCF calculations and (2) direct evaluation of PES is important to obtain accurate fundamental frequencies.

We also proposed an approximated proper condition given by Eqs. (43) and (46) with $m = 0$ for practical application of MD. Only normal mode analysis is required to set up that condition. Nevertheless, the quality of such a classical frequency is also as reliable as the second-order perturbation theory in quantum mechanics as indicated by Eq. (51). Computational cost of direct-MD with such an initial condition can be lower than the second-order perturbation theory for large molecules such as $C_{18}H_{12}$ as we demonstrated because analytical anharmonic PES such as QFF is not required in direct-MD. A disadvantage of MD is it may be impossible to calculate the frequencies of certain modes because of the resonances between different modes.

References

1 K. Yagi, T. Taketsugu, K. Hirato and M. S. Gordon, *J. Chem. Phys.*, 2000, **113**, 1005–1017.
2 K. Yagi, C. Oyanagi, T. Taketsugu and K. Hirato, *J. Chem. Phys.*, 2003, **118**, 1653–1660.
3 K. Yagi, M. Keçeli and S. Hirata, *J. Chem. Phys.*, 2012, **137**, 204118.
4 J. O. Jung and R. B. Gerber, *J. Chem. Phys.*, 1996, **105**, 10332–10348.
5 O. Christiansen, *Phys. Chem. Chem. Phys.*, 2007, **9**, 2942–2953.
6 O. Christiansen, *Phys. Chem. Chem. Phys.*, 2012, **14**, 6672–6687.
7 D. Oschetzki, M. Neff, P. Meier, F. Pfeiffer and G. Rauhut, *Croatica Chemica Acta*, 2012, **85**, 379–390.
8 J. M. Bowman, T. Carrington and H.-D. Meyer, *Mol. Phys.*, 2008, **106**, 2145–2182.

9 D. Begue, P. Carbonniere and C. Pouchan, *J. Phys. Chem. A*, 2005, **109**, 4611–4616.
10 P. Cassam-Chenaï and J. Liévin, *Int. J. Quantum Chem.*, 2003, **93**, 245–264.
11 M. Keçeli and S. Hirata, *J. Chem. Phys.*, 2011, **135**, 134108.
12 M. R. Hermes, M. Keçeli and S. Hirata, *J. Chem. Phys.*, 2012, **136**, 234109.
13 M. R. Hermes and S. Hirata, *J. Chem. Phys.*, 2014, **141**, 084105.
14 O. Vendrell, F. Gatti and H.-D. Meyer, *Angew. Chem. Int. Ed.*, 2009, **48**, 352–355.
15 M. Aida and M. Dupuis, *Chem. Phys. Lett.*, 2005, **401**, 170–174.
16 T. Yamada and M. Aida, *Chem. Phys. Lett.*, 2008, **452**, 315–320.
17 T. Yamada and M. Aida, *J. Chem. Phys. A*, 2010, **114**, 6273–6283.
18 M. Aida and M. Dupuis, *J. Mol. Struct.: THEOCHEM*, 2003, **633**, 247–255.
19 M. Kaledin, A. L. Kaledin and J. M. Bowman, *J. Phys. Chem. A*, 2006, **110**, 2933–2939.
20 P. L. Silvestrelli, M. Bernasconi and M. Parrinello, *Chem. Phys. Lett.*, 1997, **277**, 478–482.
21 M. Bernasconi, P. L. Silvestrelli and M. Parrinello, *Phys. Rev. Lett.*, 1998, **81**, 12351238.
22 J.-W. Handgraaf, E. J. Meijer and M.-P. Gaigeot, *J. Chem. Phys.*, 2004, **121**, 10111–10119.
23 R. Iftimie and M. E. Tuckerman, *J. Chem. Phys.*, 2005, **122**, 214508.
24 M.-P. Gaigeot, R. Vuilleumier, M. Sprik and D. Borgis, *J. Chem. Theory Comput.*, 2005, **1**, 772–789.
25 V. Buch, F. Mohamed, M. Parrinello and J. P. Devlin, *J. Chem. Phys.*, 2007, **126**, 074503.
26 M.-P. Gaigeot, *J. Phys. Chem. A*, 2008, **112**, 13507–13517.
27 A. Cimas, P. Maitre, G. Ohanessian and M.-P. Gaigeot, *J. Chem. Theory Comput.*, 2009, **5**, 2388–2400.
28 M.-P. Gaigeot, N. A. Besley and J. D. Hirst, *J. Phys. Chem. B.*, 2011, **115**, 5526–5535.
29 M. Thomas, M. Brehm, R. Fligg, P. Vöhringer and B. Kirchner, *Phys. Chem. Chem. Phys.*, 2013, **15**, 6608–6622.
30 R. G. Gordon, *Adv. Magn. Res.*, 1968, **3**, 1–42.
31 G. Herzberg, *Molecular Spectra and Molecular Structure I.*, Krieger, Florida, 1989.
32 G. Herzberg, *Molecular Spectra and Molecular Structure II.*, Krieger, Florida, 1991.
33 D. W. Noid, M. L. Koszykowski and R. A. Marcus, *J. Chem. Phys.*, 1977, **67**, 404–408.
34 C.-B. Li, Y. Matsunaga, M. Toda and T. Komatsuzaki, *J. Chem. Phys.*, 2005, **123**, 184301.
35 S. Kawai, Y. Fujimura, O. Kajimoto, T. Yamashita, C.-B. Li and T. K. M. Toda, *Phys. Rev. A*, 2007, **75**, 022714.
36 H. Waalkens, R. Schubert and S. Wiggins, *Nonlinearity*, 2008, **21**, R1–R118.
37 T. Komatsuzaki and R. S. Berry, *Adv. Chem. Phys.*, 2002, **123**, 79–152.
38 A. J. Dragt and J. M. Finn, *J. Math. Phys.*, 1979, **20**, 2649–2660.
39 R. T. Swimm and J. B. Delos, *J. Chem. Phys.*, 1979, **71**, 1706–1717.
40 E. Rosengaus and R. L. Dewar, *J. Math. Phys.*, 1982, **23**, 2328–2338.
41 G. D. Birkhoff, *T. Am. Math. Soc.*, 1917, **18**, 199–300.
42 K. Lamon, *J. Phys. A-Math. Gen.*, 1990, **23**, 3875–3884.
43 F. G. Gustavson, *Astron. J.*, 1966, **71**, 670–686.
44 D. Sugny, M. Joyeux and E. L. Sibert, III, *J. Chem. Phys.*, 2000, **113**, 7165–7177.
45 D. Sugny and M. Joyeux, *J. Phem. Phys.*, 2000, **112**, 31–39.
46 J. B. Keller, M. L. Koszykowski and R. A. Marcus, *J. Chem. Phys.*, 1977, **4**, 180–188.
47 G. Torres-Vega and J. H. Frederick, *Ann. Phys.*, 1990, **93**, 8862.
48 A. Makowski and K. Górska, *Phys. Rev. A*, 2002, **66**, 062103.
49 C. Jaffé and W. P. Reinhardt, *J. Chem. Phys.*, 1982, **77**, 5191–5203.
50 R. B. Shirts and W. P. Reinhardt, *J. Chem. Phys.*, 1982, **77**, 5204–5217.
51 L. E. Fried and G. S. Ezra, *J. Chem. Phys.*, 1987, **86**, 6270–6282.
52 G. S. Ezra, C. C. Martens and L. E. Fried, *J. Phys. Chem.*, 1987, **91**, 3721–3730.
53 D. Farrelly and T. Uzer, *J. Chem. Phys.*, 1986, **85**, 308–318.
54 E. L. Sibert, III, *J. Chem. Phys.*, 1988, **88**, 4378–4390.
55 M. L. Sage and M. S. Child, *J. Chem. Phys.*, 1989, **90**, 7257–7263.
56 G. Servizi and G. Turchetti, *Comp. Phys. Comm.*, 1984, **32**, 201–207.
57 L. E. Fried and G. S. Ezra, *J. Comp. Chem.*, 1987, **8**, 397–411.
58 L. E. Fried and G. S. Ezra, *Comp. Phys. Comm.*, 1988, **51**, 103–114.
59 H. Teramoto and T. Komatsuzaki, *J. Chem. Phys.*, 2008, **129**, 094302.
60 H. Teramoto and T. Komatsuzaki, *Phys. Rev. E*, 2008, **78**, 017202.
61 S. Y. Y. Wong, D. M. Benoit, M. Lewerenz, A. Brown and P.-N. Roy, *J. Chem. Phys.*, 2011, **134**, 094110.
62 M. W. Schmidt, K. K. Baldridge, J. A. Boatz, S. T. Elbert, M. S. Gordon, J. H. Jensen, S. Koseki, N. Matsunaga, K. A. Nguyen, S. J. Su, T. L. Windus, M. Dupuis and J. A. Montgomery, *J. Comp. Chem.*, 1993, **14**, 1347–1363.
63 M. S. Gordon and M. W. Schmidt, *Theory and Applications of Computational Chemistry: The First Fourty Years*, Elsevier, Amsterdam, 2005, pp. 1167–1189.
64 M. P. Allen and D. J. Tildesley, *Computer Simulation of Liquid*, Oxford, New York, 1987.
65 M. Dupuis, *HONDO2004*, based on HONDO95, available from the Quantum Chemistry Program Exchange, Indiana University, 2004.
66 M. J. Frisch, G. W. Trucks, H. B. Schlegel, G. E. Scuseria, M. A. Robb, J. R. Cheeseman, G. Scalmani, V. Barone, B. Mennucci, G. A. Petersson, H. Nakatsuji, M. Caricato, X. Li, H. P. Hratchian, A. F. Izmaylov, J. Bloino, G. Zheng, J. L. Sonnenberg, M. Hada, M. Ehara, K. Toyota, R. Fukuda, J. Hasegawa, M. Ishida, T. Nakajima, Y. Honda, O. Kitao, H. Nakai, T. Vreven, J. A. Montgomery, Jr., J. E. Peralta, F. Ogliaro, M. Bearpark, J. J. Heyd, E. Brothers, K. N. Kudin, V. N. Staroverov, T. Keith, R. Kobayashi, J. Normand, K. Raghavachari, A. Rendell, J. C. Burant, S. S. Iyengar, J. Tomasi, M. Cossi, N. Rega, J. M. Millam, M. Klene, J. E. Knox, J. B. Cross, V. Bakken, C. Adamo, J. Jaramillo, R. Gomperts, R. E. Stratmann, O. Yazyev, A. J. Austin, R. Cammi, C. Pomelli, J. W. Ochterski, R. L. Martin, K. Morokuma, V. G. Zakrzewski, G. A. Voth, P. Salvador, J. J. Dannenberg, S. Dapprich, A. D. Daniels, O. Farkas, J. B. Foresman, J. V. Ortiz, J. Cioslowski, and D. J. Fox, *Gaussian 09, Revision B.01*, Gaussian, Inc., Wallingford CT, 2010.
67 W. S. Benedict, N. Gailar and E. K. Plyler, *J. Phem. Phys.*, 1956, **24**, 1139–1165.

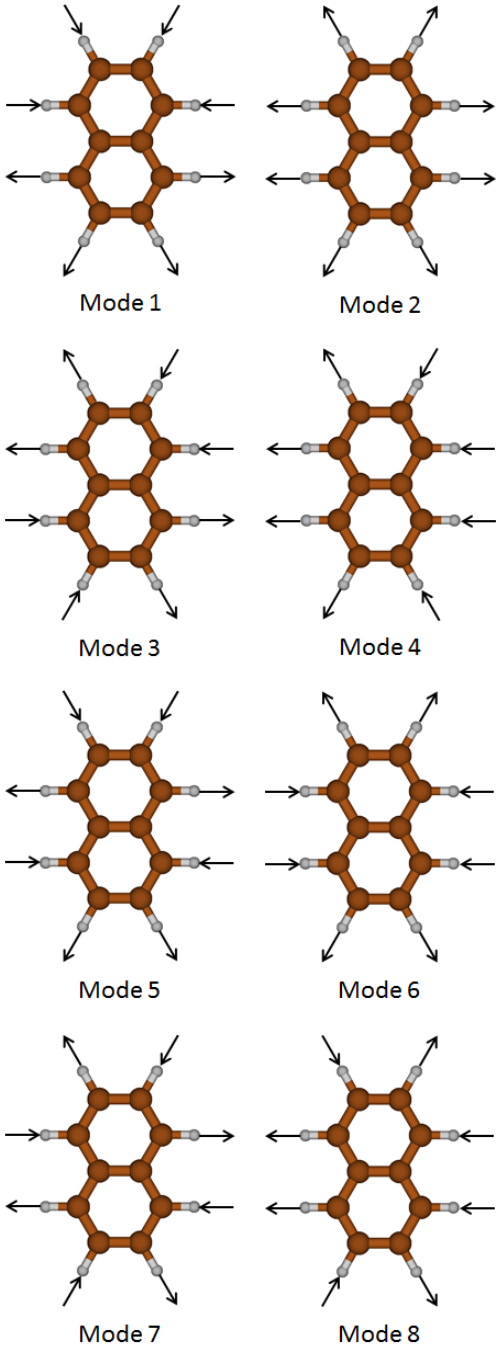

Fig. 3 C–H vibrational modes of $C_{10}H_8$, which are calculated by MD. The labels of modes are numbered from the highest harmonic frequencies.

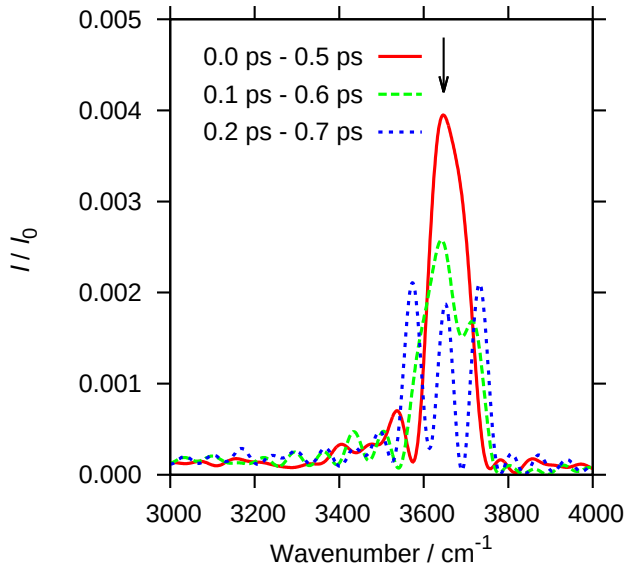

Fig. 4 Power spectrum of $C_{18}H_{12}$ from the MD calculation for $\omega_1^{cl(\infty)[0]}$. Intensity (I) is normalized by the total value (I_0). The black arrow indicates the classical frequency of 0.0 ps – 0.5 ps.

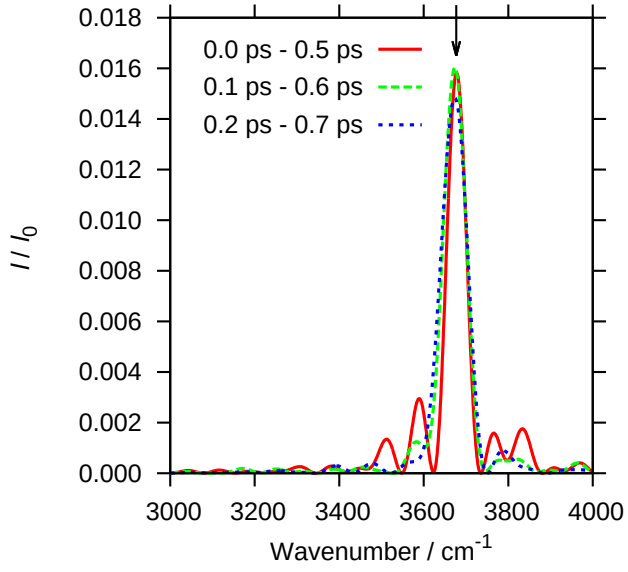

Fig. 5 Power spectrum of $C_{18}H_{12}$ from the MD calculation for $\omega_2^{cl(\infty)[0]}$. Intensity (I) is normalized by the total value (I_0). The black arrow indicates the classical frequency of 0.0 ps – 0.5 ps.

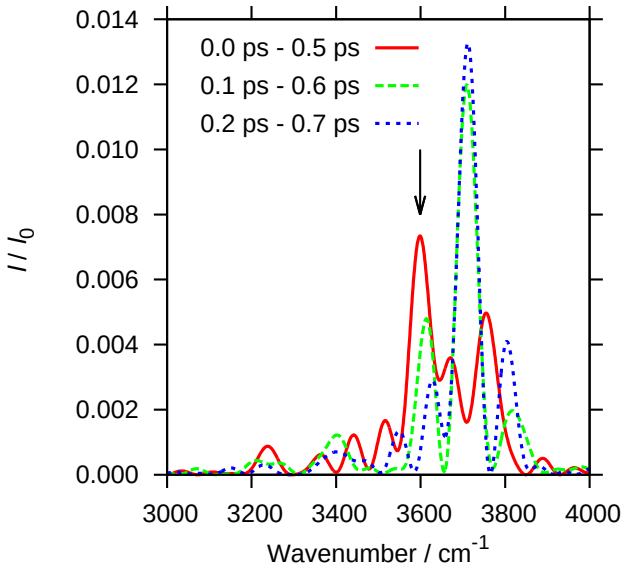

Fig. 6 Power spectrum of $C_{18}H_{12}$ from the MD calculation for $\omega_3^{cl(\infty)[0]}$ Intensity (I) is normalized by the total value (I_0). The black arrow indicates the classical frequency of 0.0 ps – 0.5 ps.

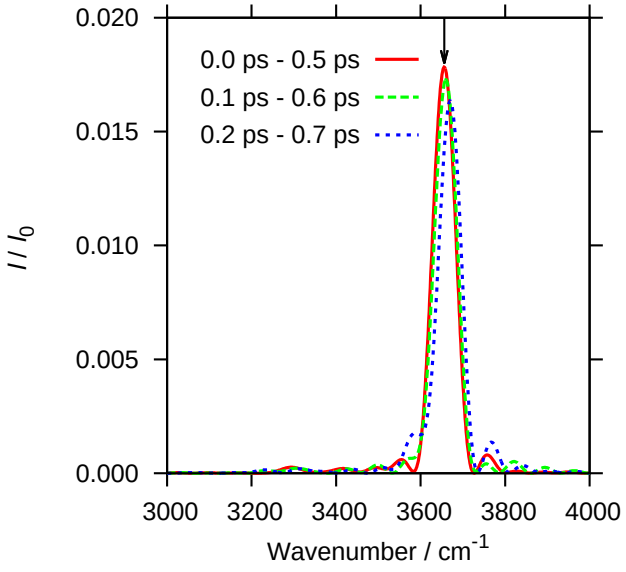

Fig. 7 Power spectrum of $C_{18}H_{12}$ from the MD calculation for $\omega_4^{cl(\infty)[0]}$. Intensity (I) is normalized by the total value (I_0). The black arrow indicates the classical frequency of 0.0 ps – 0.5 ps.